Measurement 147 (2019) 106803

Contents lists available at ScienceDirect

Measurement

journal homepage: www.elsevier.com/locate/measurement

An accurate localization method for subsea pipelines by using external magnetic fields

Chen Shili [a,b], Wu Jialin [a,b], Huang Xinjing [a,b,*], Li Jian [a,b]

[a] State Key Laboratory of Precision Measuring Technology and Instruments, Tianjin University, Tianjin, China
[b] Binhai International Advanced Structural Integrity Research Centre, Tianjin 300072, China

ARTICLE INFO

Article history:
Received 23 May 2019
Accepted 6 July 2019
Available online 15 July 2019

Keywords:
Subsea pipeline
Magnetic field
Localization

ABSTRACT

Accurate localization of subsea pipeline is the prerequisite of pipeline maintenance, reinforcement and tracking inspection. Via finite element simulations and experiments, this paper reveals the distribution characterizations of the total magnetic flux density (MFD) and the reduced MFD near the steel pipeline, and demonstrates a method for accurately positioning subsea pipeline by using the external magnetic field. The characteristic peak position of the total and reduced MFDs' components are all susceptible to the radial magnetization direction, except for the reduced MFD's norm whose peak always overlaps the projection of the pipeline axis on the magnetic measurement plane. The norms of the total and reduced MFDs are used to determine the pipeline orientation and axis position, respectively. For an 8 m long steel pipe with diameter of 8 in., when the measurement plane is 1.5 times the diameter away from the pipe, the positioning error is around 2 cm.

1. Introduction

Subsea oil and gas pipelines have long been in a harsh service environment and are prone to rupture due to corrosion, seabed displacement, and external impact. The number of subsea pipelines has rapidly increased as the exploitation of marine oil and gas resources is more and more prosperous, so the risk of rupture accidents has also greatly increased. Once a subsea pipeline leaks, it will cause very severe economic losses and environmental pollution, so it is significant to carry out routine inspection and maintenance for pipelines. Accurately positioning and tracking buried or exposed pipelines on the seabed is a prerequisite for accurate and efficient inspection, maintenance and reinforcement.

For example, when a buried subsea pipeline is to be replaced, a cofferdam needs to be constructed after piling around the upper area over the pipeline, and then the water in the cofferdam is discharged and the soil is removed, so that the damaged pipe section and its adjacent intact sections are completely exposed. If the orientation and position of the pipeline cannot be accurately determined, the construction may be blindly carried out, which will not only greatly increase the construction cost and period, but also may cause damage to the intact pipeline sections.

Subsea pipeline localization methods can be divided into three major categories: visual, acoustic and magnetic [1]. Among them, the visual method uses underwater robots AUV and ROV as carriers that are equipped with underwater cameras [2,3]. However, this method cannot detect buried pipelines and cannot be applied in turbid water regions. Acoustic methods include multi-beam echosounder, side scan sonar, shallow profiler, etc [4–7]. The detection and positioning of the subsea pipeline by acoustic methods are realized via emitting sound waves to the seabed and capturing and processing the echo signals.

The multi-beam echo sounder can acquire strip-type high-density water depth data on the line perpendicular to the vehicle course; the pipeline can be recognized and its position can be roughly determined according to the depth difference [4]. Multi-beam sounding cannot recognize a fully buried pipeline, so does side scan sonar. Side scan sonar is a more intuitive and effective way to detect bare subsea pipelines. The bare subsea pipeline shows a very strong linear shape on the sonar image, which is easier to be distinguished from other seabed features [5]. The shallow profiler is specifically designed to detect buried subsea pipelines [6,7]. Its operating frequency and power are customized for the sound to penetrate mud layers at different depths and the reflect echoes to be received by the sonar. When the soil is uniform and

* Corresponding author at: State Key Laboratory of Precision Measuring Technology and Instruments, Tianjin University, Tianjin, China.
E-mail address: huangxinjing@tju.edu.cn (H. Xinjing).

https://doi.org/10.1016/j.measurement.2019.07.031
0263-2241/

soft, the shallow profiler can detect the pipeline with very high precision. However, when the soil contains many impurities such as rocks, the contrast and accuracy of the pipeline feature on the acoustic profile image can be severely deteriorated due to the serious and complicated scattering and reflection.

The relative permeability of the subsea pipeline is much larger than 1, which can induce magnetic distribution characteristics nearby that is clearly different from the background magnetic field inside and outside the pipelines [8,9]. Among them, the magnetic field inside the pipeline has a determinate mathematical relationship with the included angle between the pipeline and the geomagnetic field, the size of the pipeline, and the magnetic permeability, and can be used to measure the pipeline orientation and trajectory [10,11]. Such kind of methods need to be carried out via an in-pipe detector, but can neither meet the accuracy requirements of pipeline maintenance nor meat the real-time requirements of pipeline tracking inspection.

Many efforts in the aspect of locating subsea pipelines by using the external magnetic fields have also been made. Based on Poisson's equation, Wang [12] et al deduced the distribution of magnetic anomalies of a long and straight pipeline under the magnetization of geomagnetic field in different directions, and used the transverse magnetic anomaly profile to determine the pipeline location. The magnetic anomaly was defined as the difference between the norm of the total magnetic field and the norm of the background magnetic field. The location deviation of the pipeline is related to the ambient field declination and the pipeline azimuth, but the mathematical relationship is unknown. Liu Yong [13] et al tried using mobile magnetometer array to obtain the magnetic field near the pipeline and use magnetic anomaly gradient to locate the pipeline. Because the magnetometers were too sparse and few, the magnetic anomaly and its gradient of the pipeline were not thoroughly and accurately captured and presented. Chen Jun [14] et al used the derived formula of magnetic gradient in a well above a pipeline to determine the burying depth and horizontal position of the pipeline through forward simulation and statistical analysis. The horizontal positioning deviation is very large and susceptible to the pipeline diameter. Guo [15] et al used the vertical magnetic field and its analytical signals to locate one section of pipe, two parallel pipes, and two cross pipes. The analytical signals were obtained via differential operation on the vertical magnetic component along the horizontal and vertical directions, which increased the difficulty of field data acquisition and introduced new errors. Yang [16] et al utilized the symmetry of the transverse magnetic anomaly distribution to roughly determine the horizontal position of a pipeline by using the extremum of the magnetic anomaly or its gradient. This method requires manual evaluation of the symmetry of the magnetic anomaly curve, which is not automatic and intelligent.

In this paper, a method for accurately positioning subsea pipeline via measuring the magnetic field distribution outside the pipeline is proposed. The norm of the total magnetic field density (MFD) is used for orientation measurement, while the norm of the reduced MFD instead of the norm difference of the total and reduced MFD is used for determining the position of the pipeline axis. The total and reduced MFDs outside the pipeline under different magnetizations are calculated via finite element simulations in order to select suitable magnetic variables for determining the position of the pipeline axis. The magnetic characterizations when the pipeline is in different directions are revealed in order to select suitable magnetic variables for determining the pipeline orientation. Based on the simulation results, implementation method and corresponding algorithm for precise orientation and localization of the pipeline are proposed. Magnetic measurement experiments are carried out to verify the validity of the simulation results and the proposed pipeline localization method.

2. Finite element simulations

Finite element simulation model is established as shown in Fig. 1. An 8 m steel pipe is deployed in the air domain. The pipe size is the same as the experimental pipe. Its outer diameter is 219 mm and wall thickness is 6 mm. The air domain size is 15 m × 5 m × 5 m and the surface of the air domain is configured as the external magnetic flux density. The air domain size is determined when the size increases the simulation results no longer change. The pipe is placed in the x-y plane with an included angle β to the x axis. The origin of the coordinate system is at the center of the pipe. Background magnetic field is the geomagnetic field $\mathbf{B_b} = (B_{bx}, B_{by}, B_{bz})$. The domains are meshed under an "Extremely fine" size configuration. The angle between the radial component $\mathbf{B_r}$ of the geomagnetic field and the z axis is θ.

Two sets of simulations are performed: (1) Different background magnetic fields with different magnitudes and directions in order to select the magnetic variables that should be adopted for pipeline axis localization; (2) Different pipeline orientations in order to determine suitable magnetic variables and magnetic measurement schemes for pipeline orientation measurement. Since the pipe is completely axisymmetric, the axial component of the background magnetic field has no effect on the magnetic anomaly characteristics, so only the influence of the radial component needs to be considered. Different radial ambient magnetic fields mean different radial magnetizations. It is necessary to study the influence of both the magnitude with θ constant and the direction of the radial component on the magnetic anomaly. Changes of θ mean that the angle between the measuring plane and the radial component is different and the magnetic anomaly characteristics may change.

2.1. Background fields with different magnitudes and directions

In practice, measuring the magnetic field above a subsea pipeline is carried out in the horizontal plane. The components of the background magnetic field in the radial and axial directions may

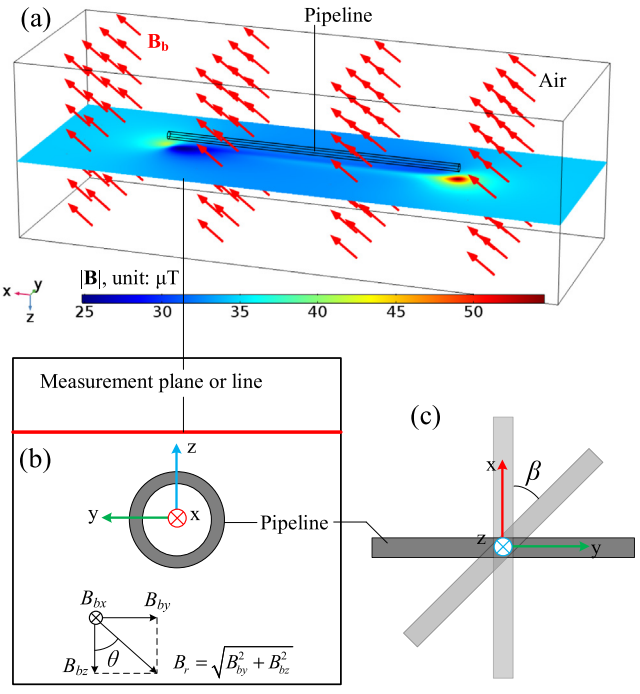

Fig. 1. Simulation model and key parameters to be studied.

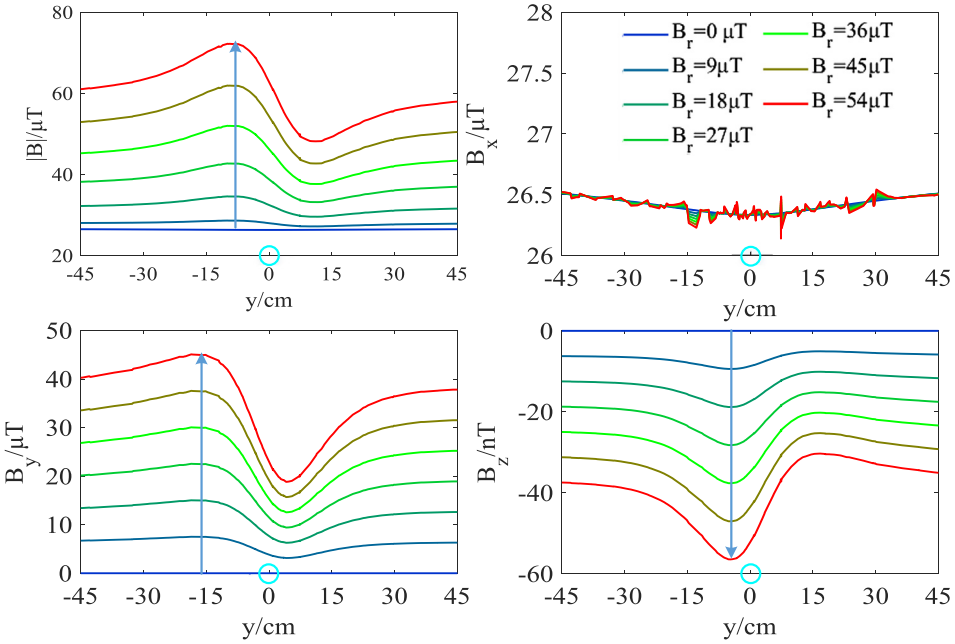

Fig. 2. Profiles of the total MFD over a pipe when θ is constant, $B_a \neq 0$, and B_r is swept.

vary as the pipeline direction changes. Since the pipeline is axisymmetric and long enough relative to its diameter, the axial magnetization does not cause a magnetic anomaly change in the measurement plane. The magnetic anomalies caused by the radial magnetizations in different directions will have different projections on the same measurement plane. Variations in intensity and direction of the radial magnetization will result in significant changes in the magnetic anomalies. To prove this conjecture, the magnitude and direction of the radial ambient field will be swept separately.

The radial magnetic intensity B_r is swept with θ set to be a fixed value of 45° (θ can also be other values). The three components and norms of the total and reduced MFDs are observed by taking a horizontal measurement line that is perpendicular to the pipeline, and the results are shown in Figs. 2 and 3. It can be seen that the shape and the peak/valley position of each curve are the same, which are independent of B_r magnitude. However, the curve amplitude gradually becomes larger as B_r increases. The total MFD, including its components and norm, deviates from the top of the pipe; while the peak of the norm of the reduced MFD is always right above the pipeline, independent of B_r, although the peak/valley positions of its components deviate a lot from the top of the pipeline.

In order to study the effect of radial magnetization direction on the characteristics of magnetic measurement curves, θ is swept from 0° to 90° with B_r in each simulation being the same, 20 μT, or other

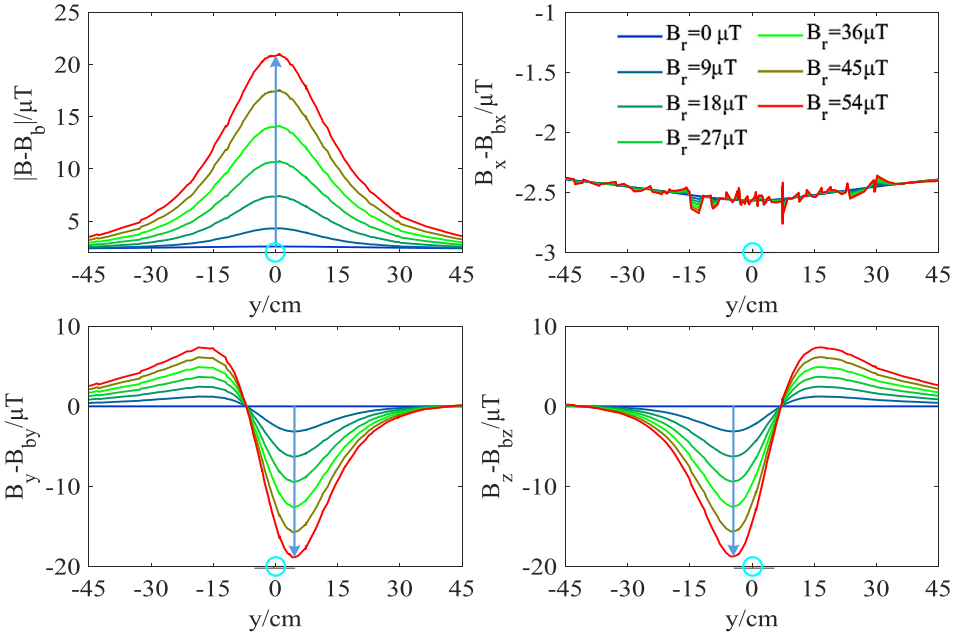

Fig. 3. Profiles of the reduced MFD over a pipe when θ is constant, $B_a \neq 0$, and B_r is swept.

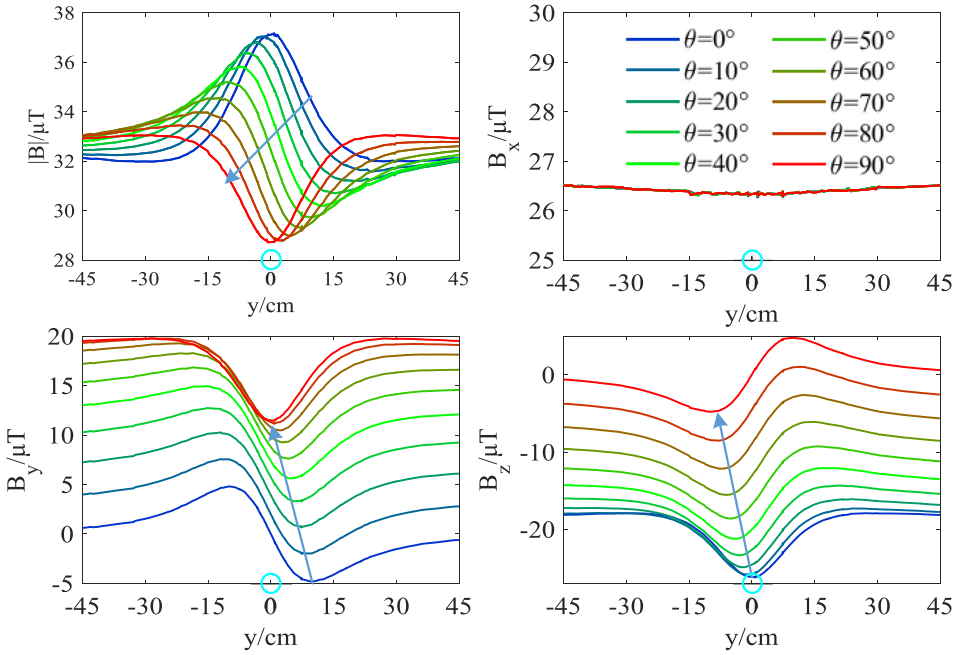

Fig. 4. Profiles of the total MFD over a pipe when B_r is constant, $B_a \neq 0$, and θ is swept.

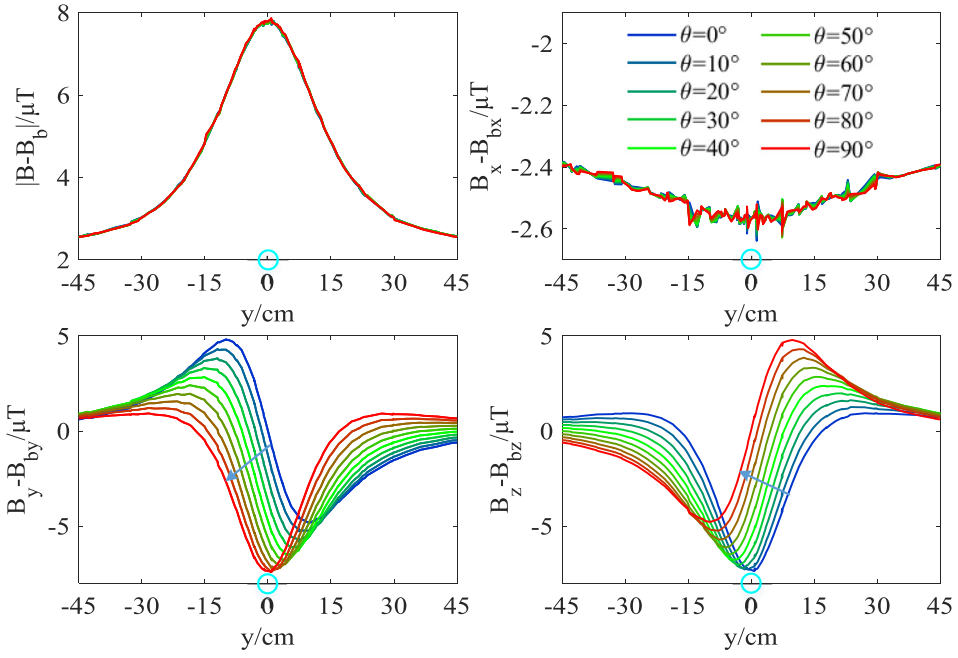

Fig. 5. Profiles of the reduced MFD over a pipe when B_r is constant, $B_a \neq 0$, and θ is swept.

values. The three components and norms of the total and reduced MFDs are observed by taking a horizontal measurement line that is perpendicular to the pipeline, and the results are shown in Figs. 4 and 5. It can be seen from Fig. 4 that as θ increases from 0° to 90°, the distribution shape of the total MFD significantly changes: (1) Its norm changes from even symmetry to odd symmetry and then back to even symmetry, and its peak gradually becomes valley; (2) Its component B_y changes from odd to even symmetry and B_z changes from even symmetry to odd symmetry; (3) The characteristic valleys of these two components shift to the left, and the DC offsets go up, although the position of the pipe has not changed.

In contrast, as shown in Fig. 5, the distribution shape of the norm of the reduced MFD does not change as θ goes up, and all the curves overlap with each other. The peak of the norm of the reduced MFD is always right above the pipeline, and the peak magnitude is dependent on B_r magnitude. The component B_y-B_{by} changes from odd symmetry to even symmetry, and the component B_z-B_{yz} changes from even symmetry to odd symmetry. The characteristic valleys of the two components shift left, but the DC offsets do not noticeably change. However, the peak of any component may deviate from the pipe axis when the radial magnetization direction changes due to the pipeline orientation changes, so the

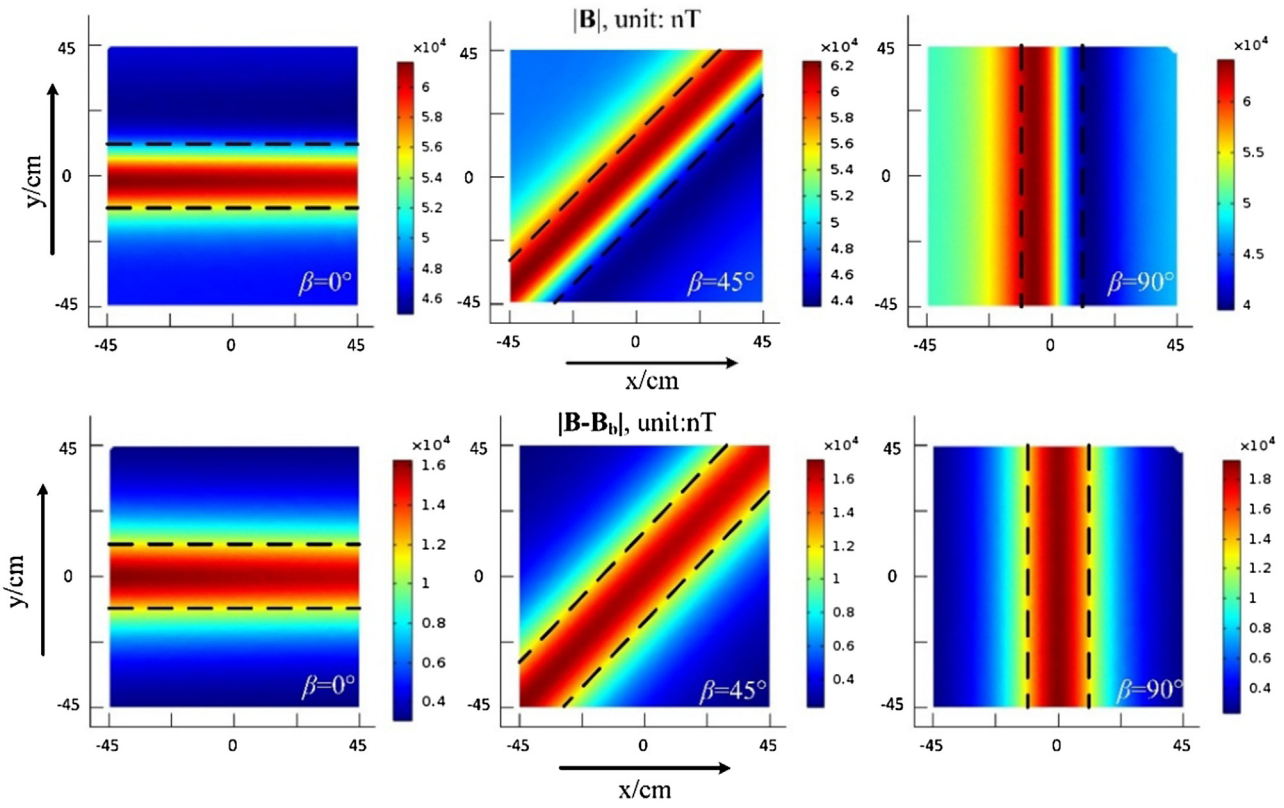

Fig. 6. Total and reduced MFD distributions above pipes with different directions.

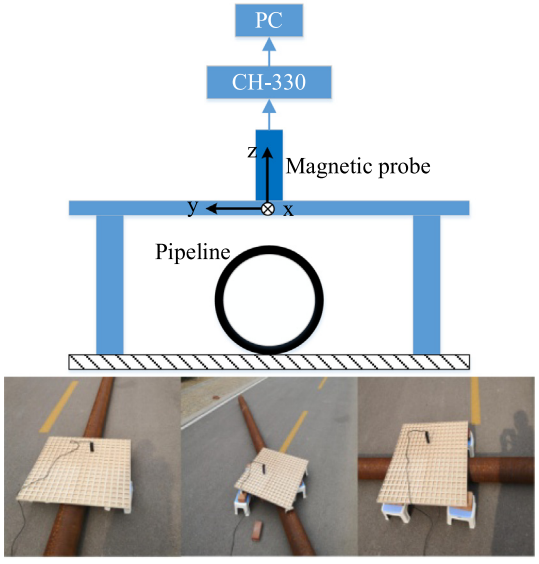

Fig. 7. Experiment apparatus.

position of the pipe axis cannot be indicated by the components. Therefore, only the norm of the reduced MFD can be used to precisely locate the pipeline.

2.2. Pipes in different directions

Keep the background magnetic field constant, place the pipe along different directions, and perform finite element simulation to simulate the measurement process of a real pipe's external magnetic field. Let the coordinate axis x be east, y be west, and z be upward. The pipes are placed along the east, northeast, and north, correspondingly, $\beta = 0°$, 45°, and 90°. The geomagnetic field is set equal to the value that is measured outdoor at Tianjin: $B_{bx} = 28.9$ μT, $B_{by} = 7.5$ μT, $B_{bz} = -39.3$ μT. The magnetic measurement plane is horizontal with an area of 90 cm × 90 cm right above the pipe. The norms of the total and reduced MFDs of the three cases are measured separately.

The results are shown in Fig. 6, where the dashed lines denote actual edges of the pipe projections on the magnetic measurement plane. It can be clearly seen that the norms of both the total and reduced MFDs around the pipe can accurately characterize straight characteristics and orientations of the pipes. However, the peak position of the former has deviations from the actual pipe position in different extents when the pipe orientation changes, while the peak position of the latter is always right above the pipe with no deviation for all pipe orientations.

Following conclusions can be drawn from the simulation results above: the peak position of the norm of the total MFD can accurately determine the pipe orientation, but cannot correctly indicate the horizontal position of the pipe; the localization deviation is related to the radial magnetization direction, but the mathematical relationship is unknown. The norm of the reduced MFD can accurately indicate both the pipe orientation and the axis position, as its peaks can always overlap the pipe axis. The noise of the reduced MFD obtained by the simulation are very small, only containing mesh noise. When the actual magnetic field is measured, the signal-to-noise ratio (SNR) of the reduced MFD is even lower than that by simulation due to unstable movement and performance inconsistency of the magnetometer, which is unfavorable for pipe orientation measurement. Subsequent experiments will also demonstrate that the total MFD is smoother and more stable than the reduced MFD. Its SNR is higher, so it is more conducive of using

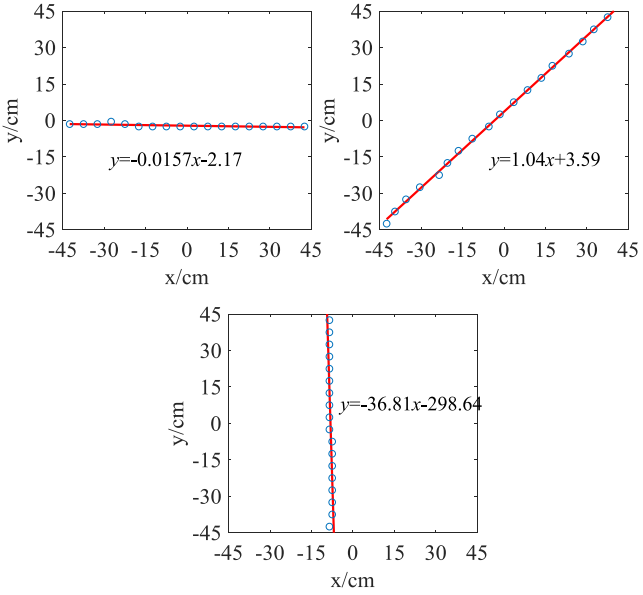

Fig. 8. Linear fitting of the peak positions on total MFD's norm profiles.

the total MFD to identify the pipe orientation. Therefore, the norm of the total MFD can be utilized to measure the pipe orientation while the norm of the reduced MFD can be used to measure the axis position. It is worth noting that in order to obtain the reduced MFD, three-dimensional magnetic measurement is required.

3. Pipeline localization method based on magnetic measurement

First, three-dimensional total MFD **B** in the plane above the pipeline is measured, and its norm |**B**| at each measuring point is calculated. Second, measure the local geomagnetic field $\mathbf{B_b}$ after the magnetometer is taken far away from the pipeline or the pipeline is removed, and calculate the reduced MFD's norm $|\mathbf{B}-\mathbf{B_b}|$. Finally, execute the following algorithms on these measured data to obtain the direction and axis position of the pipeline. Magnetometric array can be either plane array or moving linear array. Taking an N * N array as an example, the data processing algorithms are described as follows. Here, the x and y axes belong to the measuring coordinate system, which are the layout direction of the sensor array or the moving direction of a single sensor.

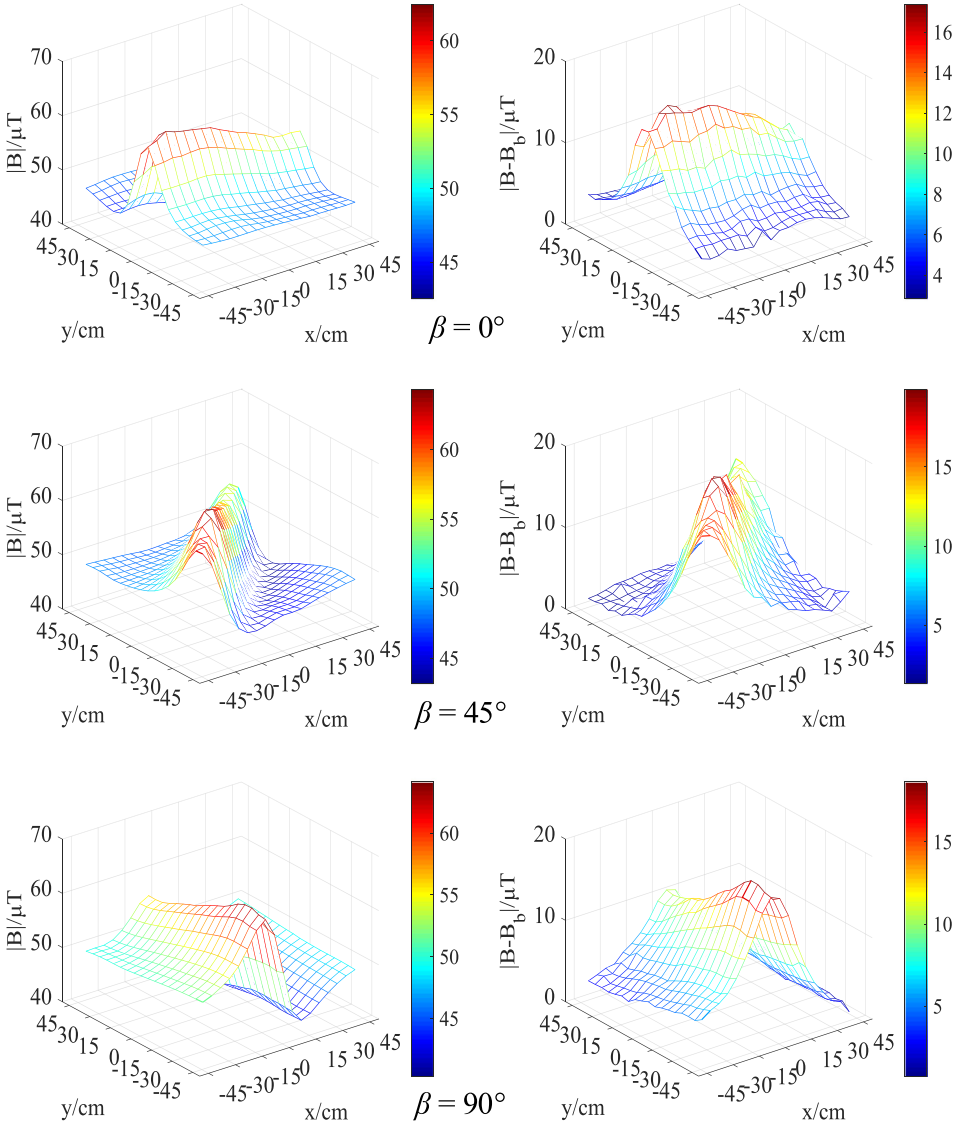

Fig. 9. Measured total MFD (left) and reduced MFD (right) over a pipe in different directions.

(i) Use $\{|\mathbf{B}|\}_{N\times N}$ to calculate the pipeline direction:
  (1) Binarization: Search for the global maximum of the matrix $\{|\mathbf{B}|\}_{N\times N}$,$B_m$; assign 1 to elements less than $0.9 * B_m$ and assign 0 to the remaining elements, and then logical matrix is obtained.
  (2) Judge whether the pipeline direction is inclined to the x axis or y axis: calculate the number of all-zero rows n_1 and the number of all-zero columns n_2 of the logical matrix; if $n_1 > n_2$, the pipeline is inclined to the x axis, and in the next step, peak detection along the y axis will be executed; if $n_1 < n_2$, the pipeline is inclined to the yaxis, and in the next step, peak detection along the x axis will be executed.
  (3) Peak detection: the peak coordinates (x_{pi}, y_{pi}) of each row or column can be obtained based on parabolic fitting [10].
  (4) Linear fitting: By linear fitting with equation $y = k * x + b$ for those peak coordinates (x_{pi}, y_{pi}), the slope k can be obtained, and the pipeline direction $\beta = \arctan(k)$.

(ii) Use $\{|\mathbf{B} - \mathbf{B_b}|\}_{N\times N}$ to calculate the position of the pipeline axis:
  (5) Transverse measurement line extraction: establish a new coordinate system in the same measurement plane with its x' axis perpendicular to the pipeline, y' axis being the pipeline axis, and the origin at the center of the measurement plane; extract the norm of the reduced MFD from $\{|\mathbf{B} - \mathbf{B_b}|\}_{N\times N}$ on the lines parallel to x' and perpendicular to the pipeline via interpolation.
  (6) Peak detection: Detect the peak of each line with the peak position denoted as x_i', and calculate its average $\bar{x}$; the position equation of the pipeline is finally determined as $y = k * x + \bar{x}/\cos(\beta)$.

4. Experiments

Experiment apparatus is shown in Fig. 7. Three-dimensional magnetometer CH-330F was used to measure the external MFD above the pipeline. The magnetometer has a measurement range of 0-100μT and a resolution of 0.01nT. The outer diameter of the steel pipe used in the experiment is 219 mm, the wall thickness is 6 mm, and the length is 8 m, which are the same as in the simulation. The measuring platform is supported above the pipe and the measuring area is 0.9 m × 0.9 m. There are 324 (18*18) square grooves in total on the measuring plane for fixing the probe of the magnetometer. In three experiments, the pipes were placed in the north, west, and northwest directions respectively. The probe was sequentially placed in each of the grooves in the platform, and the three components of the total MFD at each measuring point were recorded. For each measurement, the magnetic signal was recorded for a duration of a few seconds and its average was employed to reduce the error. Finally, the pipe was removed and the local geomagnetic field was measured.

5. Results and discussions

The experimental results are shown in Fig. 8. It can be seen that the experimental and simulation results are very similar, which can confirm the correctness of the simulation results. It is worth noting that the distribution of the norm of the total MFD is very smooth, no matter whether it is obtained via simulation or experiment. The norm of the reduced MFD obtained via experiment has many noises and its distribution is very rough. This is because the reduced MFD is the difference between the total MFD and the ambient field, therefore it is much smaller than the total MFD and its SNR is lower. Each time the magnetic probe is moved and re-fixed, its posture is not exactly the same. The norm of the total MFD is used to calculate the pipe direction; The result is shown in Fig. 9. It can be seen that these peak points are closely distributed on a straight line with very low dispersion, therefore it can be used to reliably indicate the pipe orientation.

Based on previous analysis results, the norm of the reduced MFD were used to position the pipe axis. In order to further reduce the random error, two algorithms for determining the pipe axis position are proposed: (1) The data is interpolated on each

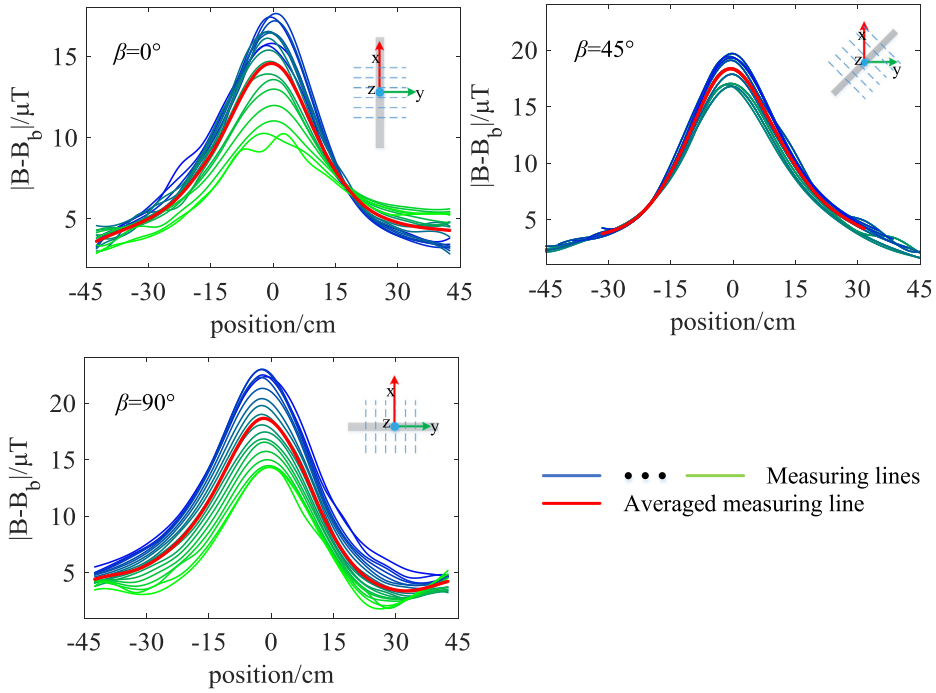

Fig. 10. Reduced MFDs on lines perpendicular to the pipe and their average.

Table 1
Positioning errors of pipeline axis, $\bar{x}$, unit: cm.

Methods	Scenarios		
	$\beta = 0°$	$\beta = 45°$	$\beta = 90°$
1#	−0.5	−0.5	−1.5
2#	−0.44	−0.62	−1.75
3#	−1	−1.5	−2.5

extracted line perpendicular to the pipe; these extracted measurement lines are summed together and averaged along the pipe axis, obtaining one averaged curve; the peak of the curve is detected and located to determine the pipe axis's position. (2) Find the peak position of each line perpendicular to the pipe, and then calculate the average of the peak positions to locate the pipe axis.

The measuring lines perpendicular to the pipeline and their averages are shown in Fig. 10. Table 1 lists the results of the two data averaging methods and the result without averaging. The maximum error is 2.5 cm without averaging. The maximum errors of the two averaging method are 1.5 cm and 1.75 cm respectively; the positioning error is reduced by 40% and 30% respectively. The experimental results demonstrate that the accuracy of the proposed method can satisfy the requirements by piling construction and underwater robot following pipeline.

6. Conclusion

This paper has revealed the distribution characterizations of the components and norms of the total and reduced MFDs near the steel pipeline. Based on this, a method for accurately locating the subsea pipeline by using the external magnetic field is proposed. The following conclusions can be obtained:

(1) The peak position of the norm and components of the total MFD and the components of the reduced MFD are all susceptible to the radial magnetization direction, except for the norm of the reduced MFD, whose peak always overlaps the projection of the pipeline axis on the magnetic measurement plane.
(2) The norms of both the total and reduced MFDs can accurately indicate the pipeline orientation, while only the norm of the reduced MFD can indicate the position of the pipeline axis with no deviation.
(3) Experiments demonstrate that the proposed method can accurately measure the orientation and horizontal position of a steel pipe. For an 8 m long steel pipe with diameter of 8 in., when the measurement plane is 1.5 times the diameter away from the pipeline, the positioning error is around 2 cm.

Declaration of Competing Interest

The authors declared that they have no conflicts of interest to this work.

Acknowledgments

This work is supported by National Natural Science Foundation of China (No. 61773283, 51604192) and Project funded by China Postdoctoral Science Foundation (No. M630271).

References

[1] Yang Min, Song Sheng, Wang Fang, et al., Discussion methods of buried submarine pipeline detection and application of new technology, Mar. Sci. 39 (6) (2015) 129–132.
[2] Petraglia F R, Campos R, José Gabriel R C. Gomes, et al. Pipeline tracking and event classification for an automatic inspection vision system. 2017 IEEE International Symposium on Circuits and Systems (ISCAS). IEEE, 2017.
[3] Zeng Wenjing, Xue Yuru, Wan Lei, et al., Robotics vision-based system of autonomous underwater vehicle for an underwater pipeline tracker, J. Shanghai Jiaotong Univ. (Science) 46 (2) (2012) 178–183.
[4] V.H. Fernandes, A.A. Neto, D.D. Rodrigues, Pipeline inspection with AUV, Acoustics in Underwater Geosciences Symposium, IEEE, 2016.
[5] A. Bagnitsky, A. Inzartsev, A. Pavin, et al., Side scan sonar using for underwater cables & pipelines tracking by means of AUV. Underwater Technology (UT), in: 2011 IEEE Symposium on and 2011 Workshop on Scientific Use of Submarine Cables and Related Technologies (SSC), IEEE, 2011, pp. 1–10.
[6] S.R. Griffin, S.C. Kuhn, K. Benjamin, Parametric sub-bottom profiler for AUVs, Sea Technol. 46 (7) (2005) 31–35.
[7] W.M. Tian, Integrated method for the detection and location of underwater pipelines, Appl. Acoust. 69 (5) (2008) 387–398.
[8] Huang Xinjing, Chen Shili, Guo Shixu, Zhao Wei, Jin Shijiu, Magnetic charge and magnetic field distributions in ferromagnetic pipe, Appl. Comput. Electromagnet. Soc. J. 28 (8) (2013) 737–746.
[9] Huang Xinjing, Chen Guanren, Yu. Zhang, Xu. Li Jian, Chen Shili Tianshu, Inversion of magnetic fields inside pipelines: modeling, validations, and applications, Struct. Health Monit. An Int. J. 17 (1) (2018) 80–90.
[10] Xinjing Huang, Shili Chen, Shixu Guo, Xu. Tianshu, Qianli Ma, Gregory S. ShijiuJin, Chirikjian, A 3D localization approach for subsea pipelines using a spherical detector, IEEE Sens. J. 17 (6) (2017) 1828–1836.
[11] Zhao Wei, Huang Xinjing, Chen Shili, Zeng Zhoumo, Jin Shijiu, A detection system for pipeline direction based on shielded geomagnetic field, Int. J. Press. Vessels Pip. 113 (2014) 10–14.
[12] F. Wang, Y. Song, L. Dong, et al., Magnetic anomalies of submarine pipeline based on theoretical calculation and actual measurement, IEEE Trans. Magn. 55 (4) (2019) 1–10.
[13] Y. Liu, Y.F. Zhang, H. Yi, The new magnetic survey method for underwater pipeline detection, Appl. Mech. Mater. 239–240 (2012) 338–343.
[14] Chen Jun, Chen Zeyuan, Yang Chuan, Borehole magbetic gradient mehod based on detection of deep underground pipeline, Earth Sci. 12 (2015) 2110–2118.
[15] Z. Guo, D. Liu, Q. Pan, et al., Vertical magnetic field and its analytic signal applicability in oil field underground pipeline detection, J. Geophys. Eng. (2015).
[16] Yang Xiaodi, Liu Zhenwen, Chun Minghao, Luo Xiaoqiao, Research of magnetic survey of seabed pipeline, Hydrographic Surv. Charting 39 (01) (2019) 52–56.